Published online 1 July 2022

Nucleic Acids Research, 2022, Vol. 50, No. 13 ***7739–7750***
https://doi.org/10.1093/nar/gkac554

Repurposing CRISPR RNA-guided integrases system for one-step, efficient genomic integration of ultra-long DNA sequences

Zhou-Hua Cheng[1], Jie Wu[2], Jia-Qi Liu[2], Di Min[2], Dong-Feng Liu[1,2,*], Wen-Wei Li[2,*] and Han-Qing Yu[2,*]

[1]School of Life Sciences, University of Science and Technology of China, Hefei, 230026, China and [2]Department of Environmental Science and Engineering, University of Science and Technology of China, Hefei 230026, China

Received March 29, 2022; Revised June 14, 2022; Editorial Decision June 14, 2022; Accepted June 16, 2022

ABSTRACT

Genomic integration techniques offer opportunities for generation of engineered microorganisms with improved or even entirely new functions but are currently limited by inability for efficient insertion of long genetic payloads due to multiplexing. Herein, using *Shewanella oneidensis* MR-1 as a model, we developed an optimized CRISPR-associated transposase from cyanobacteria *Scytonema hofmanni* (ShCAST system), which enables programmable, RNA-guided transposition of ultra-long DNA sequences (30 kb) onto bacterial chromosomes at ∼100% efficiency in a single orientation. In this system, a crRNA (CRISPR RNA) was used to target multicopy loci like insertion-sequence elements or combining I-SceI endonuclease, thereby allowing efficient single-step multiplexed or iterative DNA insertions. The engineered strain exhibited drastically improved substrate diversity and extracellular electron transfer ability, verifying the success of this system. Our work greatly expands the application range and flexibility of genetic engineering techniques and may be readily extended to other bacteria for better controlling various microbial processes.

INTRODUCTION

Genetic engineering techniques have greatly advanced our understanding and manipulation of living organisms. Especially, the recent development of *in vitro* recombination and gene editing techniques allow us to customize a living organism's genetic sequence (1,2), thereby endowing it with entirely new physiology and functions. To realize the expression of foreign genes in host microbes, plasmid-based system or chromosomal integration strategy is commonly employed (3,4). Plasmids can be conveniently used for metabolic engineering of cells and expression of recombinant proteins. However, antibiotics have to be added in such processes in order to prevent plasmid loss, which not only cause secondary environmental pollution but also complicate the final product separation (5,6). Furthermore, this technique may lead to microbial metabolic unbalance and suffer from plasmid instability, making it difficult for expressing natural metabolic gene cluster up to tens of kilobases (kb) (7). These drawbacks of conventional plasmid-based system have motivated the search for antibiotic-free genetic engineering techniques (8). One possible strategy is to raise the importance of plasmids to host microbes by means such as expressing anti-toxin genes for detoxification of toxins from a toxin–antitoxin operon (9) or the origin of replication-encoded plasmid replication inhibitor in growing cells (10), so that plasmid can be introduced without dosing antibiotics (11). However, this approach is still time-consuming, labor-intensive, and is challenged by cell-to-cell variation and inability for expression of long natural metabolic genes (12,13).

Compared with gene expression from plasmids, chromosomal integration allows more efficient genomic insertion of the metabolic genes and pathways due to its high stability in gene expression and minimized cell-to-cell variation (4,13). Multiple genomic integration approaches have been developed to date (4). By adopting these genomic integration methods, the pace to obtain excellent traits of important functional microbes can be accelerated. For example, recombinase-assisted genome engineering enables the integration of alginate metabolic pathway into the genome of *Escherichia coli*, thereby realizing the integration of long DNA constructs (14). In addition, serine recombinase-mediated site-specific integration has been adopted to successfully integrate natural product synthesis genes (up to 10–100 kb) into the genome of actinomycetes (15,16). Nevertheless, these methods for long DNA constructs inte-

*To whom correspondence should be addressed. Tel: +86 551 63607907; Fax: +86 551 63607907; Email: dfl@ustc.edu.cn
Correspondence may also be addressed to Wen-Wei Li. Tel: +86 551 63607592; Fax: +86 551 63607592; Email: wwli@ustc.edu.cn
Correspondence may also be addressed to Han-Qing Yu. Tel: +86 551 63601592; Fax: +86 551 63601592; Email: hqyu@ustc.edu.cn

gration still involve complicated operations and have been mainly used for model microbes (4,14,17). Effective and convenient approaches for integration of ultra-long DNA constructs into the microbial genome are still on urgent demand.

The recent advances of clustered regularly interspaced short palindromic repeats (CRISPR)-based technologies (1,18) are bringing new dawn to solve this problem. In particular, the combination of CRISPR technology and homologous recombination allows for efficient gene deletion, integration and single nucleotide modification (19). However, this technology can only be utilized for integration of a limited cargo size of about 10 kb (20,21). A transposon-encoded CRISPR-Cas system (INTEGRATE), consisting of DNA-targeting complex Cascade and the transposition protein TniQ, was designed to achieve RNA-mediated insertion of donor DNA with variable lengths at a fixed distance downstream of target DNA sequences (22). Although a marker-free and highly accurate DNA integration of about 10 kb at ∼100% efficiency can be achieved by the optimized single-plasmid INTEGRATE system (23), it is difficult for genomic integration of oversized DNA cassettes due to the huge size of such a system. Recently, another CRISPR-associated transposase from cyanobacteria *Scytonema hofmanni* (ShCAST) has emerged and exhibit efficiently for DNA insertion in *E. coli* (24). ShCAST consists of the type V-K CRISPR effector (Cas12k) and Tn7-like transposase subunits (TnsB, TnsC and TniQ) and catalyzes the RNA-guided DNA transposition by insertion of DNA 60 to 66 bp downstream of the protospacer adjacent motif (PAM) sequences (24,25). This system contains two plasmids (pHelper and pDonor) and directs targeted DNA integration with a lower fidelity than the INTEGRATE system. Although the feasibility and reliability of this system were only verified in restricted species, the ultrasmall-sized pDonor provides a huge space for ShCAST system to integrate oversized DNA cassettes over 10 kb in microbes (24).

Therefore, this work aims to develop an optimized ShCAST system for high-efficient integration of ultra-long DNA sequences onto bacterial chromosomes in a single orientation by using *Shewanella oneidensis* MR-1 as a model. To enable site-specific integration of kilobase-sized DNA sequences in *Shewanella* species and other microbes, we first developed an optimized ShCAST system for highly efficient large-scale gene insertion in *S. oneidensis* MR-1. Next, the feasibility of single-step multiplexed or iterative DNA integration into the same cells and the potential for integrating up to 30 kilobases in bacteria using the optimized ShCAST system was explored. Lastly, we examined whether this system could function as an effective genetic tool to successfully break the two important bottlenecks in *S. oneidensis* MR-1 for practical applications.

MATERIALS AND METHODS

Plasmid construction

The *J23119* promoter-driving crRNA cassette, *lac* promoter-driving tnsB-tnsC-tniQ-Cas12k-tracrRNA expression cassette, the I-SceI recognition site and the I-SceI Endonuclease expression cassette were synthesized by General Biosystems Co., China. These expression cassettes were assembled into the pYYDT plasmid (26) to form the pHelper. The original pDonor plasmid (contains chloramphenicol resistance gene flanked by the transposon left end and right end) was synthesized by General Biosystems Co., China according to the sequences reported (24). The glucokinase (*glk*; ZMO0369), fructokinase (*frk*; ZMO1719), glucose facilitator (*glf*; ZMO0366) genes and 30 kb DNA fragment were amplified from the *Zymomonas mobilis* ZM4. The sucrose metabolism gene clusters (*cscY-cscB-cscA*), the flavin synthesis gene clusters, the violacein synthesis gene clusters, extracellular amylase-encoding gene (*amyE*), and 20 kb DNA fragment were amplified from *Pseudomonas protegens* Pf-5, *Bacillus subtilis* strain 168, *Lactococcus lactis* subsp. cremoris NZ9000, *Chromobacterium violaceum* ATCC 12742 and *Pseudomonas aeruginosa* PAO1, respectively. These DNA fragments were integrated into pDonor plasmid via Gibson assembly method (27). The plasmids used in this work are listed in Supplementary Table S2. The complete sequence of the optimized ShCAST system is provided in the supporting information.

General transposition assays

Plasmids pHelper and pDonor could be co-transformed into *S. oneidensis* MR-1 by conjugation. In brief, *E. coli* WM3064 containing pHelper or pDonor was cultured in LB medium supplemented with 50 μg/ml diaminopimelic acid and appropriate antibiotics at 37°C. The wild-type and engineered strains of *S. oneidensis* MR-1 were cultured in LB medium at 30°C. After overnight incubation, the pure cultures of *E. coli* and *S. oneidensis* were mixed in equal proportion. The cells (500 μl mixture) were then pelleted by centrifugation, re-suspended with 100 μl LB and dropped on the LB agar plates containing 50 μg/ml diaminopimelic acid. After 12-h cultivation at 30°C, the formed bacterial plaque was scraped, re-suspended with 1 ml LB and spread on LB plates supplemented with appropriate antibiotics. When required, 50 μg/ml kanamycin, 10 μg/ml chloramphenicol or 15 μg/ml gentamycin was added into the LB plates. All plates were placed 24 h in a 30 °C incubator to allow transposition to take place. The transposon events could be readily identified by PCR (Supplementary Table S3) and Sanger sequencing.

Single-step multiplexed or iterative DNA integration assays in the same cells

Single-step multiplexed DNA integration in MR-1 was conducted through constructing the pHelper with two crRNAs targeting sites S3 and S7 or a crRNA targeting ISSod10. The goal strains were obtained according to the general transposition assays described above. For iterative DNA integration in *S. oneidensis* MR-1, chloramphenicol resistance gene was initially inserted into site S3, the positive clones were cultured overnight in LB medium supplemented with 10 mM arabinose (I-SceI counter-selection) and the resulting plasmid-free strain was annonated as MR-1/Cm. Next, both pHelper with a crRNA targeting S7 and pDonor with gentamycin resistance cargo gene were introduced into MR-1 and MR-1/Cm to generate MR-1/Gm

Table 1. Strains used in this work

Strains	Relevant genotype or phenotype	Source or reference
MR-1	Wild-type	Lab stock
MR-1/S1	Insertion of chloramphenicol resistance gene at *SO_0261* in *S. oneidensis* MR-1	This work
MR-1/S2	Insertion of chloramphenicol resistance gene at *SO_0314* in *S. oneidensis* MR-1	This work
MR-1/S3	Insertion of chloramphenicol resistance gene at *SO_0986* in *S. oneidensis* MR-1	This work
MR-1/S4	Insertion of chloramphenicol resistance gene at *SO_1396* in *S. oneidensis* MR-1	This work
MR-1/S5	Insertion of chloramphenicol resistance gene at *SO_1779* in *S. oneidensis* MR-1	This work
MR-1/S6	Insertion of chloramphenicol resistance gene at *SO_2727* in *S. oneidensis* MR-1	This work
MR-1/S7	Insertion of chloramphenicol resistance gene at *SO_2917* in *S. oneidensis* MR-1	This work
MR-1/S8	Insertion of chloramphenicol resistance gene at *SO_3715* in *S. oneidensis* MR-1	This work
MR-1/S9	Insertion of chloramphenicol resistance gene at *SO_3980* in *S. oneidensis* MR-1	This work
MR-1/S10	Insertion of chloramphenicol resistance gene at *SO_4591* in *S. oneidensis* MR-1	This work
MR-1/11.4 kb	Insertion of violacein synthesis gene cluster (11.4 kb) cloned from *Chromobacterium violaceum* ATCC 12472 at *SO_0986* in *S. oneidensis* MR-1	This work
MR-1/S3-22.6 kb	Insertion of 22.6 kb gene fragment cloned from *Pseudomonas aeruginosa* PAO1 at *SO_0986* in *S. oneidensis* MR-1	This work
MR-1/S3-31.7 kb	Insertion of 31.7 kb gene fragment cloned from *Zymomonas mobilis* ZM4 at *SO_0986* in *S. oneidensis* MR-1	This work
MR-1/IS	Insertion of chloramphenicol resistance gene at four IS repeats in *S. oneidensis* MR-1	This work
MR-1/Sucrose	Insertion of *glf*, *glk*, *frk* and *csc* gene cluster at *SO_2917* in *S. oneidensis* MR-1	This work
MR-1/Starch	Insertion of *glf*, *glk*, *frk* and *aymE* at *SO_2917* in *S. oneidensis* MR-1	This work
MR-1/Sucrose-Rib	Insertion of flavin synthesis gene cluster at *SO_0986* in MR-1/Sucrose	This work
MR-1/Starch-Rib	Insertion of flavin synthesis gene cluster at *SO_0986* in MR-1/Starch	This work
E. coliWM3064	*thrB1004 pro thi rpsL hsdS lacZ*ΔM15 RP4-1360Δ*(araBAD)567*Δ*dapA1341::*[erm pir(wt)]	Lab stock

and MR-1/Cm-Gm, respectively. The growth of the MR-1, MR-1/Cm, MR-1/Gm and MR-1/Cm-Gm in LB medium supplemented with or without 10 μg/ml chloramphenicol and 15 μg/ml gentamycin was monitored by measuring the optical density at 600 nm (OD_{600}) using a BioTek microplate reader (Synergy HT, BioTek Ins., U.S.A.).

Carbon source utilization assays, flavins determination, and flow cytometric analysis

S. oneidensis MR-1 and MR-1/Sucrose were cultured in LB medium for 12 h, and then transferred at a ratio of 1:100 into 96-well plate containing 200 μl mineral salt medium (28) with lactate, glucose, fructose, or sucrose as the sole carbon source (20 mM). The growth curves of *S. oneidensis* MR-1 and MR-1/Sucrose were obtained by measuring the OD_{600} using a BioTek microplate reader (Synergy HT, BioTek Ins., U.S.A.). The growth of *S. oneidensis* MR-1 and MR-1/Starch in mineral salt medium containing 20 g/l starch was estimated by CFU counting. The production of α-amylase in *S. oneidensis* MR-1 and MR-1/starch was further assessed by visualization of starch degradation halos on 2% starch-containing LB plates after staining with iodine solution (29).

The flavin synthesis in *S. oneidensis* MR-1, MR-1/sucrose-Rib and MR-1/starch-Rib was determined as follows: all the strains were cultured overnight in LB medium with 10 mM IPTG (Isopropyl β-D-Thiogalactopyranoside) at 30°C. The culture supernatant was collected by centrifugation at 12 000 *g* for 2 min and its fluorescence intensity was recorded by fluorescence spectroscopy with an excitation wavelength of 440 nm and an emission wavelength of 525 nm.

The fluorescence intensity of GFP in *S. oneidensis* MR-1 was measured by a Flow Cytometer (CytExpert, Beckman Coulter Inc., U.S.A.), and the collected data were analyzed by CytExpert 2.0 software (Beckman Coulter Inc., U.S.A.).

Electrochemical tests

A MFC system was used to detect the EET abilities of *Shewanella* (Table 1). The two chambers, each with a working volume of 150 ml, were separated by a cation exchange membrane. The treated carbon felt was used as the anode and cathode materials (the anode was 1 × 1 cm, and the cathode was 2 × 2 cm). The two electrodes were connected by a 1 kΩ resistance wire. The cathodic electrolyte was composed of solution of 50 mM potassium ferricyanide in 50 mM phosphate buffer solution. The mineral medium with 20 mM lactate, glucose, frutose, sucrose or 20 g/l starch as the sole electron donor was used as the anodic electrolyte. High-purity nitrogen gas was flushed into the anode and cathode chambers to keep the anaerobic atmosphere.

S. oneidensis MR-1 and the engineered strains were cultured in LB medium for 16 h at 30 °C. The centrifuged cell pellets were washed twice with 10 ml PBS (phosphate buffered saline, pH 7.3–7.5) and re-suspended with 2 ml mineral salt medium (without carbon source). The bacterial suspension (50 ml) was subsequently added into the anode chamber at an initial optical density (OD_{600}) of 0.3. The voltage output of the MFCs inoculated with *Shewanella* strains was recorded every 10 min using a data acquisition system (USB2801, ATD Co., China). Linear sweep voltammetry (LSV), CV, and EIS analysis were conducted as described previously (26).

The three-electrode MECs (carbon felt as anode material with a specific surface area of 8 cm^2) were also adopted to evlaute the EET ability of *Shewanella* by applying a constant potential of 0.2 V (26). An electrochemical workstation (CHI1030B, Chenhua Instrument Co., China) served as the potentiostat. *S. oneidensis* MR-1 and the engineered strains were cultured in mineral medium with different carbon sources under aerobic conditions until an OD_{600} reached 0.5. Subsequently, the cultures were directly transferred into MECs.

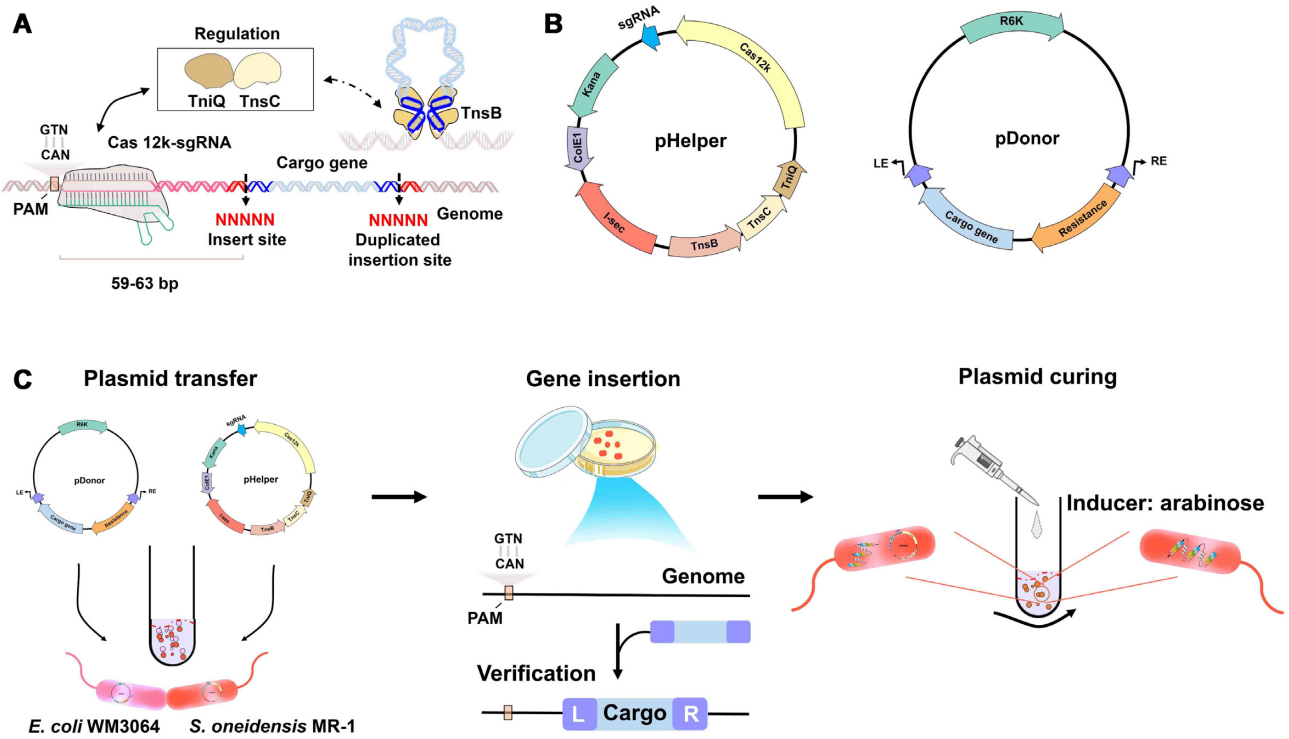

Figure 1. RNA-guided DNA integration by ShCAST system. (**A**) Model for RNA-guided DNA transposition by ShCAST system. (**B**) A two-plasmid ShCAST system encodes protein-RNA components on pHelper and the cargo gene flanked by the transposon left end (LE) and right end (RE) on pDonor. (**C**) Schematic of experiment to test for genome insertions in MR-1. Plasmids pHelper and pDonor could be co-transformed into *S. oneidensis* MR-1 by conjugation. The transposon events could be readily identified by PCR and Sanger sequencing. A I-SceI recognition site and the I-SceI Endonuclease expression cassette under the control of the arabinose-inducible araBAD promoter were integrated into the pHelper to cure the plasmids after editing. PAM: protospacer adjacent motif sequences; L: the transposon left end; R: the transposon right end.

RESULTS

Optimization of ShCAST system for high-efficiency, RNA-guided DNA integration

ShCAST system relies on the cooperation of dual plasmids (pHelper and pDonor) to precisely insert cargo gene into the host cells. The pHelper contains *J23119* promoter-driving crRNA (CRISPR RNAs) cassette and *lac* promoter-driving tnsB-tnsC-tniQ-Cas12k-tracrRNA (trans-activating crRNA) expression cassette. The R6K replicon-based pDonor contains a genetic cargo flanked by the transposon left end (LE) and right end (RE) (24). Cryogenic electron microscopic studies reveal that TnsC polymerization and TniQ interacting with TnsC define downstream transposition insertion polarity and the target-site, respectively (30). After cotransformation of pHelper and pDonor into *S. oneidensis* MR-1, the ShCAST complex made up of Cas12k, TnsB, TnsC and TniQ and guided by crRNA mediated the integration of cargo genes downstream of the PAM (Figure 1A).

We randomly selected 10 different non-essential gene sites (S1-S10) on the genome of *S. oneidensis* MR-1 and designed the corresponding crRNAs (Figure 2A, C, D, and Supplementary Figures S1 and S2, Table S1). The efficiency of the same cargo gene (chloramphenicol resistance gene) being integrated into the different target sites was evaluated through two pairs of primers. Each pair of primers contained a primer located within the transposon donor DNA and a primer adjacent to the target genomic site. We found that the integration efficiencies were above 95% in seven sites and between 50% and 80% in the other three sites (Figure 2B and Supplementary Figure S1). The lower integration efficiencies in these three sites might be originated from the poor activity of *lac* promoter in *S. oneidensis* MR-1. Moreover, integration events occurred, favoring 59 and 63 base pairs (bp) downstream of the target site in a single orientation (Figure 2C, D and Supplementary Figure S2).

We further optimize the pHelper to enable more efficient expression of the necessary protein-RNA components. To promote the expression of *gfp* in *S. oneidensis* MR-1, a panel of constitutive promoters (five endogenous promoters: *P0139*, *P3285*, *P2277*, *P0406*, *P3988*; five exogenous promoters: *Ppcn*, *Plac*, *Ptrc*, *PrpsL*, *PJ23119*) was used. Flow cytometry analysis reveals that all these constitutive promoters could work but with varied expression strengths (Figure 3A, B). We then modified *lac* promoter-driving protein–RNA expression cassette at different intensities with the three constitutive promoters (Figure 3C, low; *0139*; medium; *0406*; high: *3988*). Higher expression led to 100% integration efficiency at the S4, S6 and S7 sites (Figure 3D). The elimination of pHelper after gene integration is essential for the multi-round genome editing. To cure the plasmids after transposition, an I-SceI recognition site and the I-SecI Endonuclease (31) expression cassette under the control of the arabinose-inducible araBAD promoter were also integrated into the optimized pHelper (Supplemen-

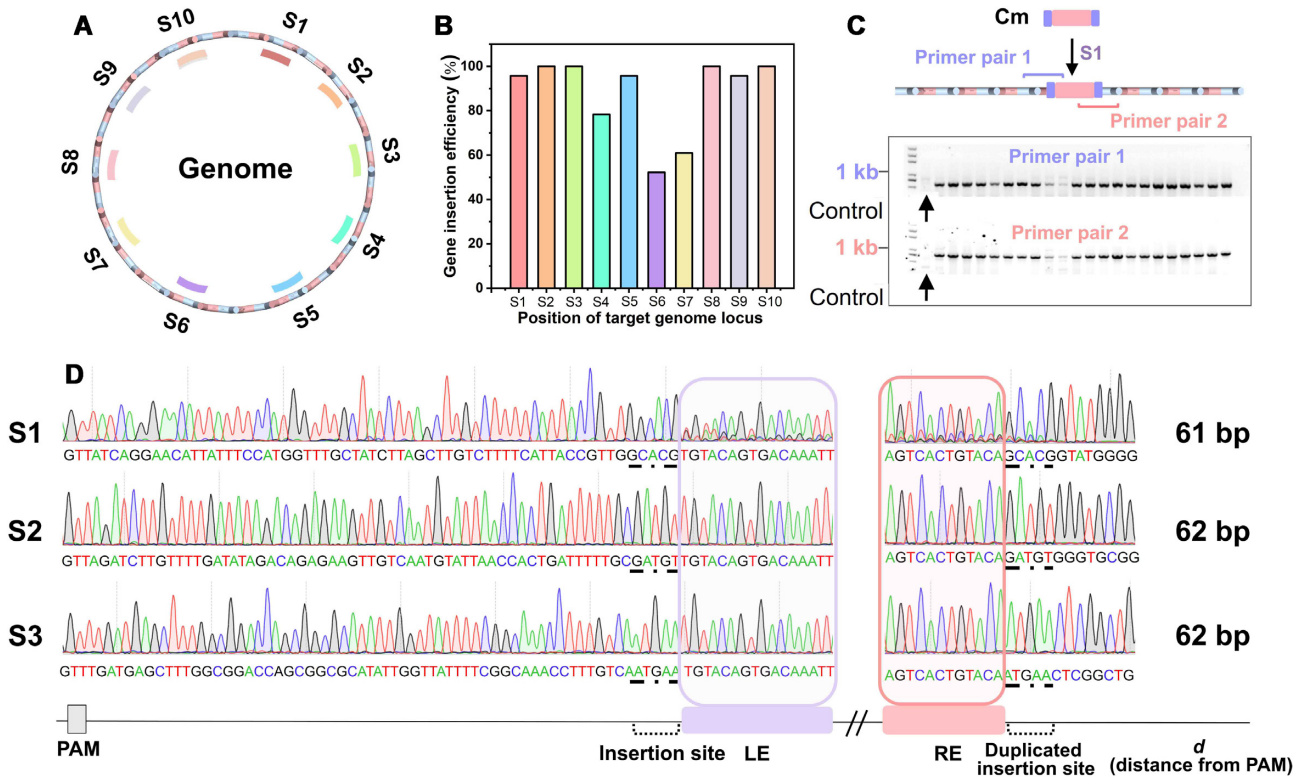

Figure 2. Gene integration at ten sites on the genome of *S. oneidensis* MR-1 by the original ShCAST system. (**A**) Schematic of 10 sites (S1, S2, S3…S10) on the genome. (**B**) Gene integration efficiencies at different sites. (**C**) PCR products with two primers pairs probing for the insertion of the cargo gene at the target site, resolved by agarose gel electrophoresis. (**D**) Sanger sequencing chromatograms for the upstream and downstream junctions of genomically integrated transposons from the experiments with crRNA-S1, crRNA-S2 and crRNA-S3. LE and RE elements are highlighted and the duplicated insertion sites denoted. Data in (B) are shown as mean ± s.d. for $n = 3$ biologically independent samples.

tary Figure S3a), which enabled the complete elimination of the pHelper after arabinose induction (Supplementary Figure S3b). All these results demonstrate that the optimized ShCAST system can achieve efficient, large-scale gene insertion in *S. oneidensis* MR-1. This optimized system was used for the subsequent tests.

Single-step multiplexed or iterative DNA integration into the same cell using the optimized ShCAST system

Multiple insertions with a high specificity in distinct genomic regions are highly desired for metabolic engineering (32,33). However, traditional approaches like integrating of multiple FLP recombinase target sites beforehand into the genomes of microbes are cumbersome (34). To resolve this problem, we firstly evaluated the amenability of the optimized ShCAST system for single-step multiplexed DNA integration. Two crRNAs were employed to target the S3 and S7 sites simultaneously, but only a single insertion in S3 site was obtained.

Insertion-sequence (IS) elements, typically <3 kb in length, contain transposase-encoding genes for their independent transposition (35). A large and diverse population of IS elements have been identified in the genome of *S. oneidensis* MR-1 and are considered to play critical roles in modulating its genome plasticity (36). Thus, we designed crRNA targeting IS elements for single-step multiplexed DNA integration in the genome of *S. oneidensis* MR-1. The ISSod10 with four identical copies in *S. oneidensis* MR-1 was chosen as the IS element. A 2 kb cargo gene (chloramphenicol resistance gene) was inserted into four IS repeats simultaneously at ∼100% efficiency (Figure 4A, B, Supplementary Figure S4). Given the high copy numbers of some IS elements in *S. oneidensis* MR-1 (ISSo1 and ISSo4 with 49 and 53 copies, respectively) and other microbes (36), our results imply a great application potential of the optimized ShCAST system for single-step multiplexed DNA integration in various microbes. Briefly, the ShCAST system could achieve multiple insertions at a high efficiency when the target sites harbor repeated sequences.

The amenability of the optimized ShCAST system for iterative integration events was also evaluated. After isolating a clonal strain (MR-1/Cm) containing the S3 site-specific insertion (chloramphenicol resistance gene), we cured the plasmid and reintroduced the ShCAST system into the strain MR-1/Cm to generate another insertion (gentamicin resistance gene) at S4 site (Figure 4C). The growth of the resulting strain (named as MR-1/Cm-Gm) in the Luria–Bertani (LB) medium in the presence of chloramphenicol or/and gentamicin was monitored. It exhibited a slightly lower OD_{600} than the wild-type and the strain MR-1/Cm after 24-h cultivation. Chloramphenicol inhibited the growth of the wild-type but did not affect the MR-1/Cm-Gm and MR-1/Cm. However, only the strain MR-1/Cm-

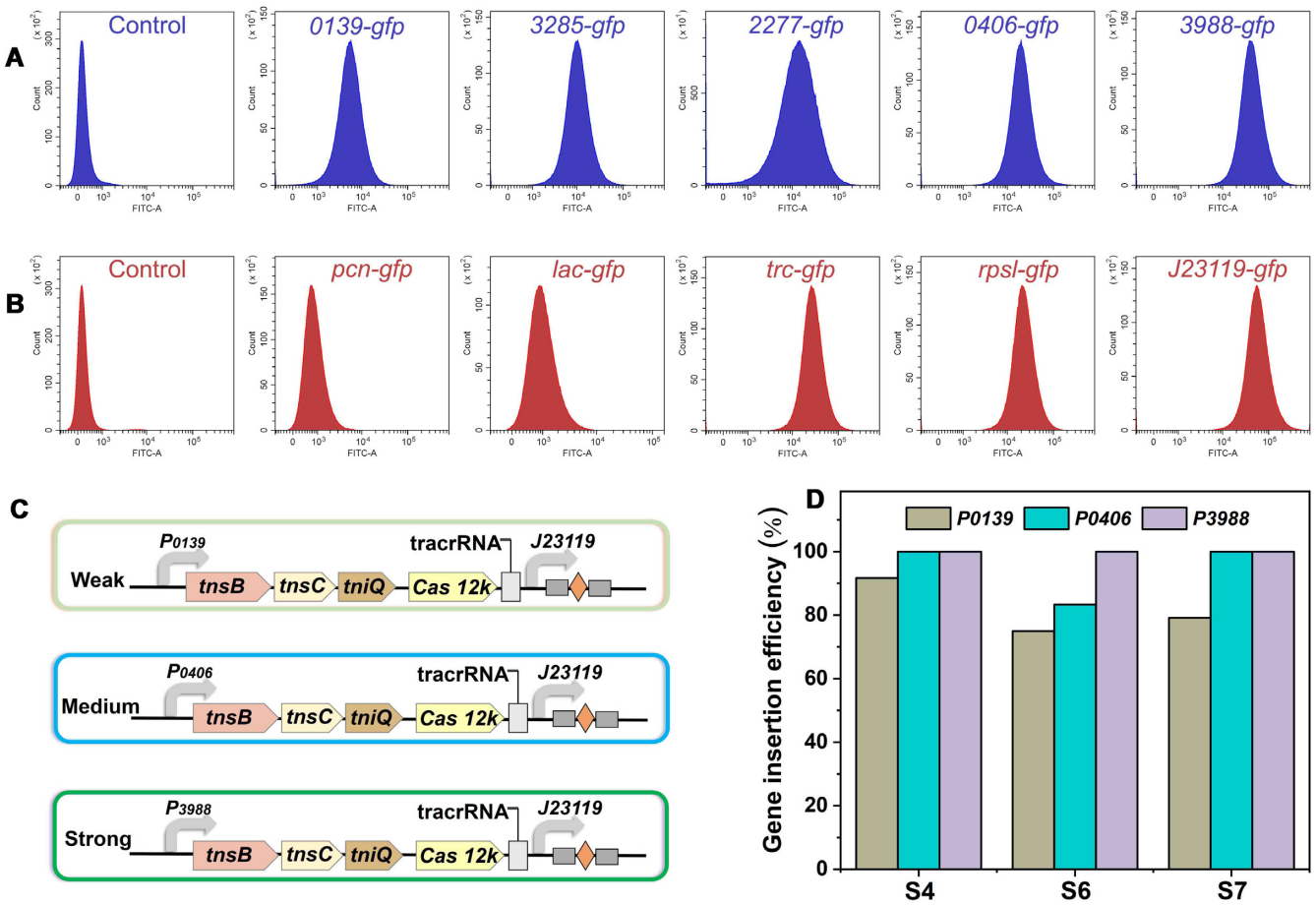

Figure 3. Optimization of ShCAST system. Characterizations of the expression intensities of the (**A**) five endogenous and (**B**) exogenous promoters by using GFP as the reporter gene. Schematics of three pHelper plasmids. (**C**) Three promoters with varying intensities (low; 0139; medium; 0406; high: 3988) were selected to drive the expression of *tnsB-tnsC-tniQ-Cas12k-tracrRNA* cassette. The *J23119* promoter was selected to drive the expression of crRNA. (**D**) Gene integration efficiencies at sites S4, S6 and S7 with the three ShCAST systems. Data in A, B and D are shown as mean ± s.d. for $n = 3$ biologically independent samples.

Gm could grow in the LB medium containing gentamicin or gentamicin plus chloramphenicol (Figure 4D). These results confirm that the optimized ShCAST system enabled the single-step multiplexed and efficient iterative DNA insertions into *S. oneidensis* MR-1.

Targeted insertion of ultra-long fragments of DNA

The ShCAST system has been used for targeted insertion of a 10 kb DNA fragment in *E. coli* (24). In order to show more intuitively that the optimized ShCAST system can change bacterial traits by introducing large segments of exogenous DNA, we inserted the violacein biosynthesis gene cluster from *Chromobacterium violaceum* ATCC 12472 into the S3 site of MR-1 (Figure 5C). The obvious color change of the strain from red to purple, with the patterns of panda and letters drawn on the plates, suggests that the insertion was successful (Figure 5A,B).

This system also enabled more efficient integration of larger fragments of DNA than the previously reported methods (24). After modification of the pDonor to mobilize payloads of 22.6 or 31.7 kb DNA fragment, we used a total of seven pairs of primers located inside the cargo gene or at the junction between the target site and cargo gene for integration verification (Figure 5D, E). Results show that the 20 or 30 kb DNA fragment was integrated into the S3 site of *S. oneidensis* MR-1 at ∼100% efficiency by using the optimized ShCAST system (Figure 5F).

Broadening the carbon source utilization spectra and enhancing the extracellular electron transfer ability of *S. oneidensis* MR-1

The genus of *Shewanella* hold a great potential for enhanced environmental remediation and bioenergy production applications due to their unique extracellular electron transfer abilities (26,37) but are currently restricted by their narrow spectrum of feedstocks and limited extracellular electron transfer (EET) efficiency (38). *S. oneidensis* MR-1 could utilize some three-carbon substrates only like lactate and pyruvate for anaerobic respiration, which severely limits their application niches (28). In break this limitation, we introduced the glucose- and fructose-utilization pathway into *S. oneidensis* MR-1 by using the optimized ShCAST system (Figure 6A). Two key genes encoding glucokinase and 6-phosphofructokinase in glycolytic pathway

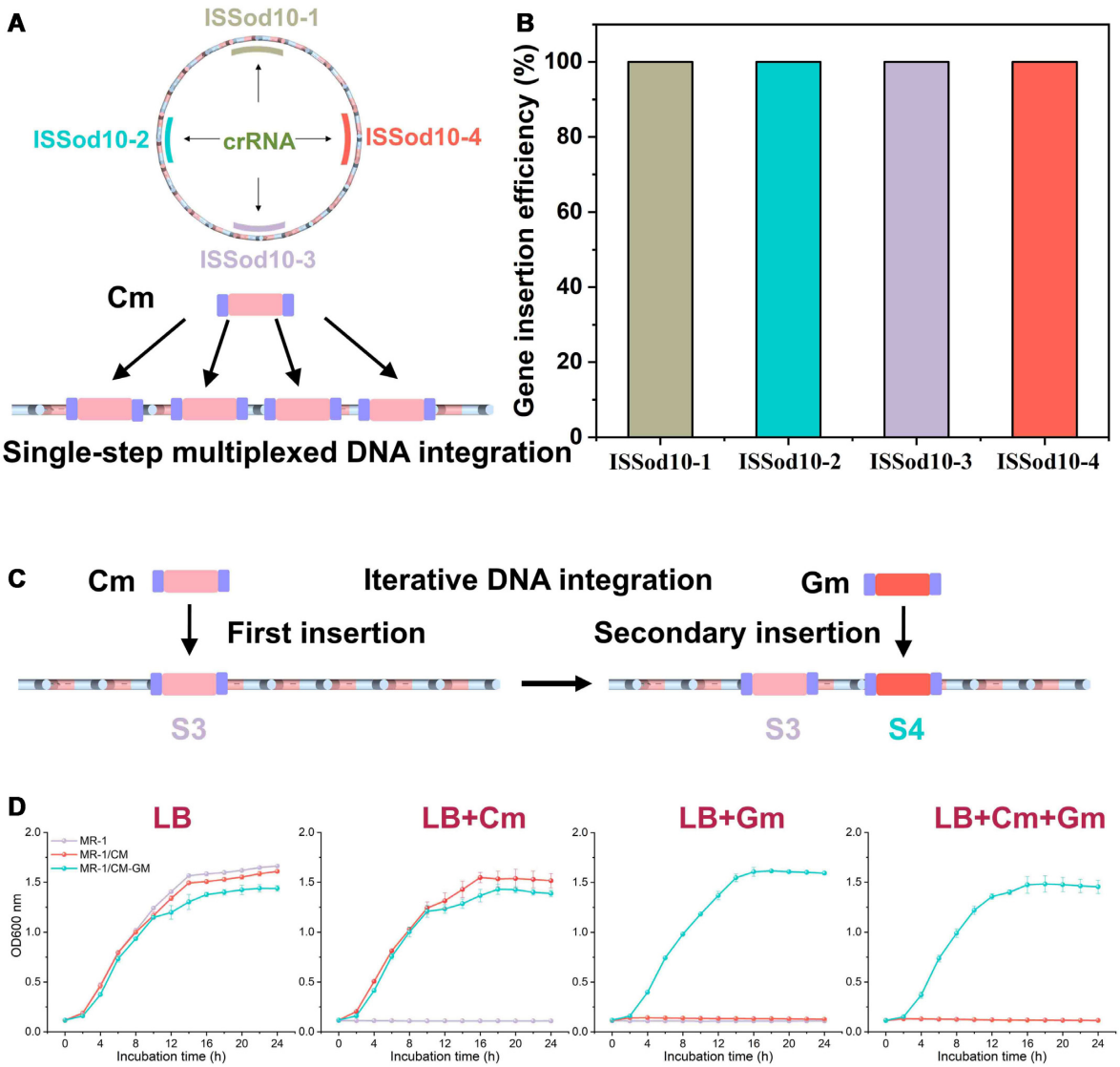

Figure 4. Single-step multiplexed or iterative DNA integration into the same cell using the optimized ShCAST system. (**A**) Schematic of single-step multiplexed DNA integration. ISSod10 with four identical copies was found in *S. oneidensis* MR-1. We designed a crRNA targeting ISSod10 for single-step integration of chloramphenicol resistance gene into four IS repeats simultaneously. (**B**) Gene integration efficiencies at four IS repeats. (**C**) Schematic of iterative integration of chloramphenicol and gentamicin resistance gene in sites 3 and 4. (**D**) The growth of *S. oneidensis* MR-1, MR-1/Cm and MR-1/Cm-Gm in LB medium in the presence of the different antibiotics. LB: LB medium only; LB + Cm: LB medium containing 10 μg/ml chloramphenicol; LB + Gm: LB medium containing 15 μg/ml gentamycin; LB + Cm + Gm: LB medium containing 10 μg/ml chloramphenicol and 15 μg/ml gentamycin. Data in b and d are shown as mean ± s.d. for $n = 3$ biologically independent samples.

were missing in the genome of *S. oneidensis* MR-1 (39). Therefore, the glucokinase (*glk*; ZMO0369), fructokinase (*frk*; ZMO1719) and glucose facilitator (*glf*; ZMO0366) genes from *Zymomonas mobilis* ZM4 under the control of the *pcn* promoter were introduced into the pDonor plasmid. The glucose facilitator could uptake glucose or fructose into the cytoplasm without requiring energy (40). Then, glucokinase and fructokinase conversed glucose and fructose into glucose-6-phosphate and fructose-6-phosphate, respectively, in the initial process of the glycolytic pathway (Figure 6A) (41). Previous studies show that, after introducing a gene cluster (*csc*) for sucrose metabolism from *Pseudomonas protegens* Pf-5, the *Pseudomonas putida* gained the ability to utilize sucrose as the sole carbon source for growth (40). This cluster consisted of four genes: *cscR* encoding the repressor protein, *cscY and cscB* facilitating sucrose transport across the cell membranes, *cscA* encoding sucrose hydrolase. Sucrose could be converted into glucose and fructose via sucrose hydrolase CscA (Figure 6A). The *cscY-cscB-cscA* cluster was also introduced into the pDonor plasmid. Therefore, utilizing the optimized ShCAST system, we successfully integrated the *glf*, *glk*, *frk* and the *cscY-cscB-cscA* cluster into the S3 site of the *S. oneidensis* MR-1 genome (Figure 6B). The resulting strain MR-1/sucrose showed a similar growth rate to the wild-type in the presence of lactate as the sole carbon source under aerobic conditions (Figure 6C). However, the wild-type could not naturally utilize sucrose, glucose and fructose, while the strain

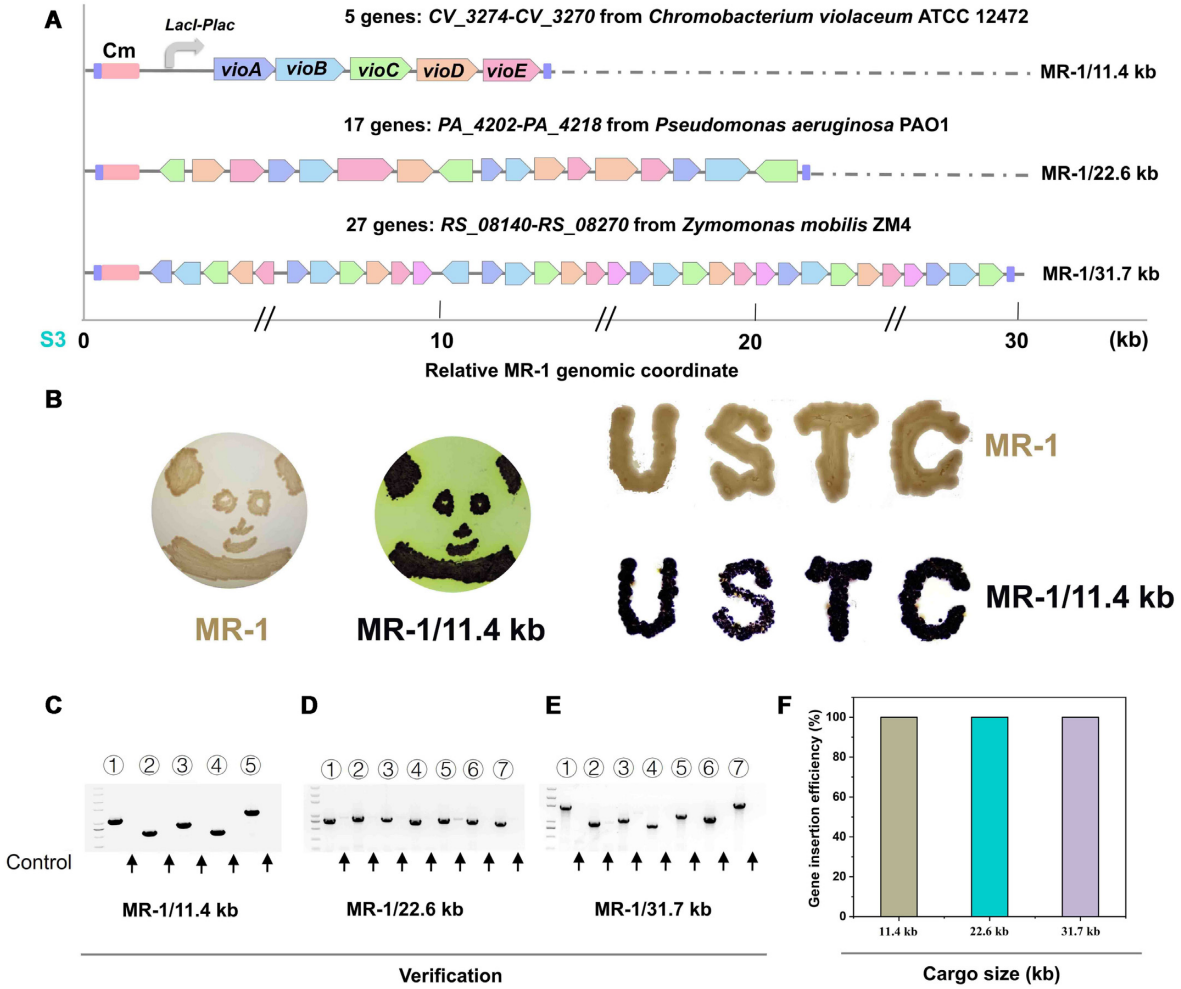

Figure 5. Targeted insertion of large fragments of DNA. (**A**) Schematic of the integration of 11.4 kb (*CV_3274-CV_3270* from *Chromobacterium violaceum* ATCC 12472, the violacein biosynthesis gene cluster), 22.6 kb (*PA_4202-PA_4218* from *Pseudomonas aeruginosa* PAO1) or 31.7 kb (*RS_08140-RS_08270* from *Zymomonas mobilis* ZM4) DNA fragment into site S3. (**B**) The patterns of panda and letters drawn on the plates using the strain MR-1 and MR-1/10.4 kb. PCR products with multiple primers pairs probing for integration of (**C**) 11.4 kb, (**D**) 22.6 kb and (**E**) 31.7 kb into site S3, resolved by agarose gel electrophoresis. Control: the genome DNA from MR-1 was used as RCR template. (**F**) Integration efficiencies of 11.4, 22.6 and 31.7 kb DNA fragment at site S3. Data in (E) are shown as mean ± s.d. for $n = 3$ biologically independent samples.

MR-1/sucrose grew well with these substrates as the sole carbon source (Figure 6D).

Starch is the most common carbohydrate in nature and can be hydrolyzed into glucose by α-amylase of bacteria (42). To further extend the substrate utilization range of *S. oneidensis* MR-1, we introduced the extracellular amylase-encoding gene (*amyE*) from *Bacillus subtilis* strain 168 controlled by the *J23119* promoter (Figure 6A) into *S. oneidensis* MR-1. The optimized ShCAST system was employed to integrate *glf*, *glk*, *frk* and *amyE* into the S3 site of the *S. oneidensis* MR-1 genome (Figure 6B). The engineered strain MR-1/Starch showed a similar growth rate to the wide type when lactate was used as the sole carbon source under aerobic conditions (Figure 6C). However, when shifting to starch carbon source, the number of MR-1/starch cells (counted by colony forming units (CFU) method) increased gradually from 2.7×10^6 to 6.1×10^8 CFU/ml after 48-h cultivation (Figure 6E), while that of MR-1 cells increased from 1.9×10^6 to only 1.0×10^8 CFU/ml (the growth was possibly caused by impurities in starch). The starch utilization by the MR-1/starch was also supported by the obvious starch degradation halo appeared after inoculation on 2% starch-containing LB plates and iodine staining (Figure 6F).

S. oneidensis MR-1 is capable of both direct electron transport via *c*-type cytochromes and indirect electron transfer using flavin as electron shuttles (26). The latter pathway accounts for about 75% of microbial extracellular electron flux to electrode (43). Therefore, we further integrated the flavin synthesis gene clusters cloning from lactic acid bacteria into the S7 site of the genome of MR-1/sucrose or MR-1/starch to enhance their EET ability (Figure 7A–C). Evaluation of the microbial EET ability in microbial electrolysis cells (MECs) at a constant anodic potential (Figure 7D–G, Supplementary Figure S7) shows a significantly higher current intensity for the MEC with the strain MR-1/Sucrose over the wide type when fed with sucrose, glucose or fructose. Similarly, the strain MR-

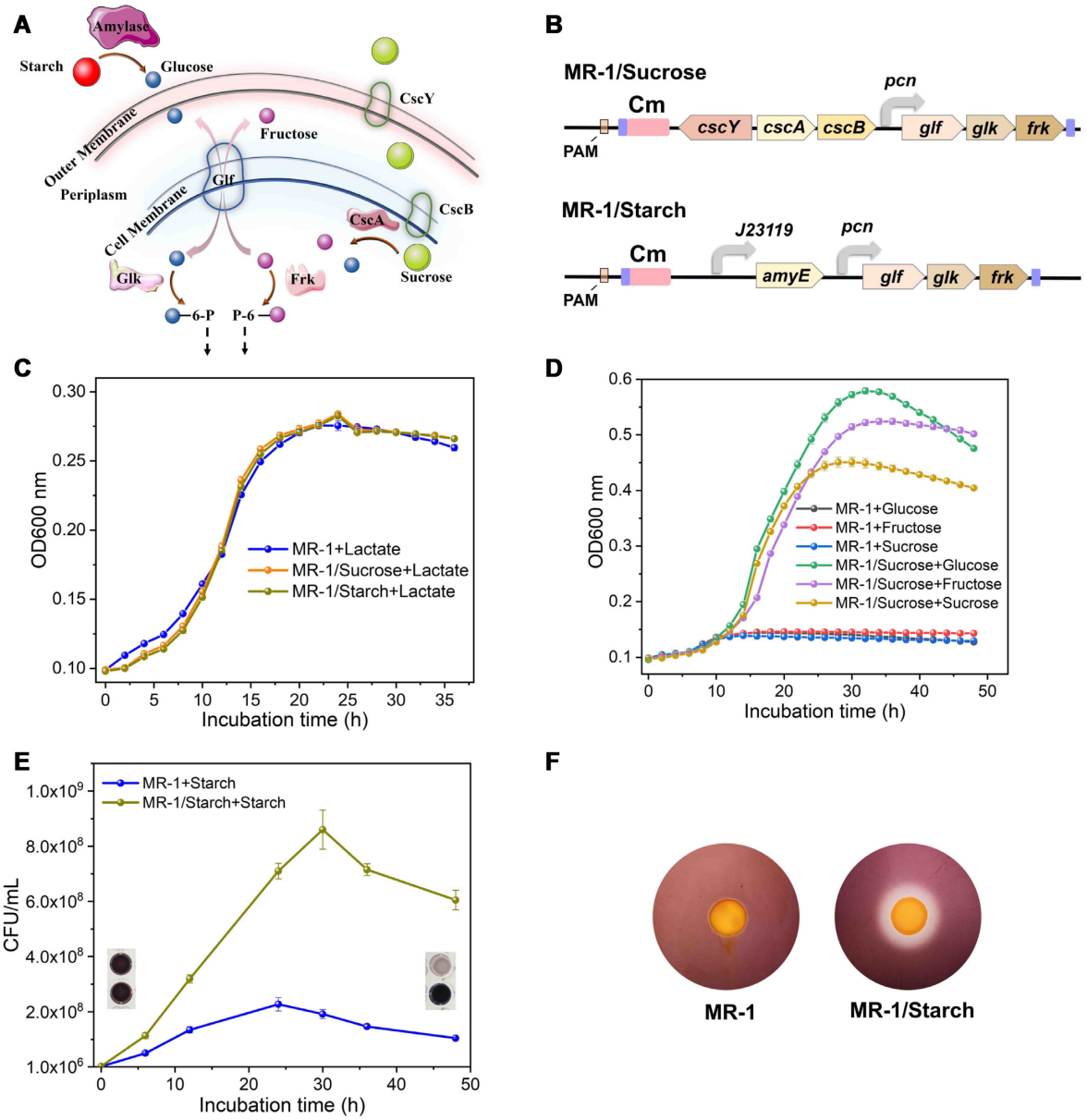

Figure 6. Broadening the carbon source utilization spectra of MR-1. (**A**) Schematic of the carbohydrate metabolism in *S. oneidensis* MR-1. The introduction of *cscY-cscB-cscA* cluster from (**B**, top) *Pseudomonas protegens* Pf-5 enabled MR-1 to grow on sucrose as the sole carbon and energy source. *cscY and cscB* facilitated sucrose transport across the cell membranes, while *cscA* encoded sucrose hydrolase. The introduction of extracellular amylase-encoding gene (*amyE*) from (B, bottom) *Bacillus subtilis* strain 168 enabled MR-1 to grow on starch as the sole carbon and energy source. The glucokinase (*glk*; ZMO0369), fructokinase (*frk*; ZMO1719) and glucose facilitator (*glf*; ZMO0366) genes from (B) *Zymomonas mobilis* ZM4 under the control of the *pcn* promoter were also introduced into *S. oneidensis* MR-1. The glucose facilitator could uptake glucose or fructose into the cytoplasm without requiring energy. Glucokinase and fructokinase converted glucose and fructose into glucose-6-phosphate and fructose-6-phosphate, respectively, in the initial process of the glycolytic pathway. (**C**) The growth curves of *S. oneidensis* MR-1, MR-1/sucrose, and MR-1/starch in mineral salt medium with lactate as the sole carbon source under aerobic conditions. (**D**) The growth curves of *S. oneidensis* MR-1 and MR-1/sucrose in mineral salt medium with sucrose, glucose, or fructose as the sole carbon source under aerobic conditions. (**E**) Evaluation of the growth of *S. oneidensis* MR-1 and MR-1/Starch in mineral salt medium with starch as the sole carbon source through the CFU method. Inset: the cultures into 96-well plates were stained with iodine solution at 0 and 48 h. Top: MR-1/Starch. Bottom: MR-1. (**F**) Observation of starch degradation halo when MR-1/starch and MR-1 were inoculated on 2% starch-containing LB plates after staining with iodine solution. Data in C, D, E and F are shown as mean ± s.d. for $n = 3$ biologically independent samples.

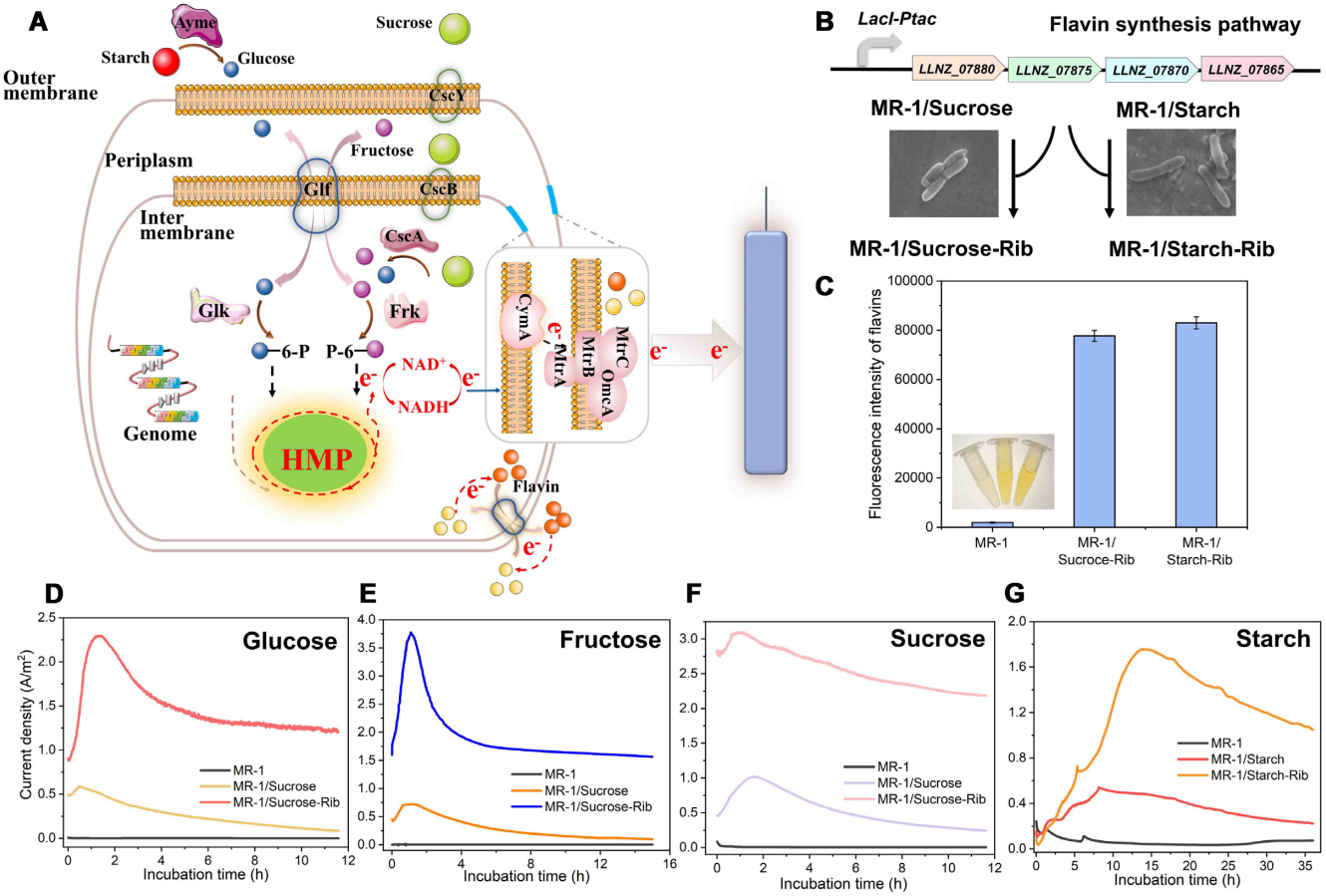

Figure 7. Enhancing the extracellular electron transfer efficiency of *S. oneidensis* MR-1. (**A**) Schematic of the extracellular electron transfer pathway in *S. oneidensis* MR-1. *S. oneidensis* MR-1 has two major electron transport mechanisms: the direct electron transport pathway based on *c*-type cytochromes and the indirect electron transport pathway based on flavin shuttles. Flavin electron shuttling accounts for about 75% of extracellular electron transfer to electrode. Therefore, we further integrated the flavin synthesis gene clusters cloning from lactic acid bacteria into the S7 site of the genome of (**B**) MR-1/sucrose or MR-1/starch to obtain the engineered strains with stronger extracellular electron transfer ability. (**C**) Comparison of the fluorescence intensities of flavins synthesized by *S. oneidensis* MR-1, MR-1/Sucrose-Rib and MR-1/Starch-Rib in LB medium. Inset: the photos of three cultures supernatant. Left: MR-1. Center: MR-1/sucrose-Rib. Right: MR-1/starch-Rib. The current densities of the MECs inoculated with *S. oneidensis* MR-1 and engineered strain when (**D**) glucose, (**E**) fructose, (**F**) sucrose or (**G**) starch was used as the sole carbon source. HMP: hexose monophosphate pathway. Data in C, D, E, F and G are shown as mean ± s.d. for $n = 3$ biologically independent samples.

1/starch could generate a stable and much larger current in the MECs than the wide type when starch was used as the sole carbon source. Moreover, the EET capabilities of the MR-1/sucrose-Rib and MR-1/starch-Rib were further improved than without flavin overexpression. The corresponding current densities of the MECs were: 3.1 A/m^2 for the MR-1/sucrose-Rib versus 1.0 A/m^2 for the MR-1/sucrose when fed with sucrose; 1.8 A/m^2 for the MR-1/starch-Rib versus 0.5 mA/m^2 for the MR-1/starch when fed with starch. Similarly, when glucose or fructose was used as the sole carbon source, the MR-1/sucrose-Rib group achieved 3.9 or 5.3 times higher current densities than the MR-1/sucrose (Figure 7D–G). Similar effects of EET enhancement by the overexpression of flavin were also demonstrated by the other engineered microbes in dual-chamber microbial fuel cells (MFCs) (Supplementary Figure S5). Cyclic voltammetry (CV) experiments (Supplementary Figure S6) and electrochemical impedance spectroscopy (EIS) analyses (Supplementary Figure S5c, f, i, l) confirm that the enhanced EET capacities of the strain MR-1/sucrose-Rib and MR-1/starch-Rib were attributed to the overproduction of flavins and lowered resistance of the electrochemical reactions on the electrodes. Together, these results validate that the optimized ShCAST system can be used as a robust tool to broaden the substrate utilization spectra and enhance the EET efficiency of *S. oneidensis* MR-1.

DISCUSSION

The optimized ShCAST system could be used for the integration of targeted DNA in microbes without need for homologous recombination and DNA double-strand breaks. In addition, it shows a higher insertion efficiency in bacterial genome than the unoptimized system, and enables one-step insertion of ultra-long DNA fragments >30 kb at ∼100% efficiency. By applying this system for multiplexed chromosomal integration, we successfully broadened the carbon source utilization spectra of *S. oneidensis* MR-1 to cover multiple carbohydrates and significantly enhanced its EET ability.

Integrases (like ICEBs1), transposases (such as Mariner, Tn5 and Tn7) and autocatalytic Group II RNA introns have been used for genomic integration (44–46). However, applications of these systems remain practically challenging because they often require prior presence of specific attachment sites in genome and large-scale screens to isolate desired clones, and generally suffer from limited cargo size (only 3–4 kb) and inconsistent integration efficiencies (from 1% to 80%). These drawbacks can be overcome by the optimized ShCAST system, which combines the programmability of CRISPR-mediated targeting with the high-efficiency, seamless integration ability of CRISPR-associated transposase and the large-cargo capability of pDonor plasmid. In addition to genomic integration, it may also be harnessed to generate programmed genomic deletions. This may be achieved through a combination of site-specific recombinases like Cre-LoxP system (47) or enable synthetic lethality screening (48) at the genome scale in microbes by generating libraries of multiplexed guide RNAs. Considering that transposons often function robustly across a broad range of hosts (49), this system could also be modified by replacing plasmid skeleton or optimizing the protein sequence and the related gene regulatory elements, so as to make the CRISPR-associated transposase systems more adaptable for the new host microbes (Supplementary Figure S8).

Nevertheless, this system still has some flaws at the present stage. First, the maximum allowable length of inserted DNA is about 30 kb. We attempted to construct the pDonor plasmid with a larger cargo size (40 or 50 kb), but failed due to the formation of a wrong plasmid with genetic sequence disorder. It seems that the maximum length of mobilize payloads depends on not only the characteristics of the ShCAST system itself but also the size of the pDonor plasmid we can build. Another challenge for the ShCAST system is the difficulty in precise, scarless point mutations or insertion on the bacterial chromosomes because the transposase machinery needs the transposon end sequences for specific recognition. However, other applications such as strain tagging and simple gene knockouts by DNA insertion are not constrained. Third, although the efficiency of single-step multicopy chromosomal integration using the ShCAST system is limited, this issue may be addressed by designing a crRNA to target multicopy loci like IS elements or combining orthogonal integrases. Finally, the lower fidelity of the ShCAST system than the INTEGRATE system has demonstrated an off-target activity and also limits its application. Addressing these challenges would require the adoption of multiple strategies to decrease its off-target editing without sacrificing on-target editing efficiency. These may include engineering the Cas12k and transposase subunits, extending the crRNA length, or using a hairpin secondary structure onto the spacer region (50). With further improvement in fidelity, the ShCAST system may offer an appealing tool for organism- and locus-specific genetic manipulation within microbial communities.

DATA AVAILABILITY

All data are available from the corresponding authors upon reasonable request.

SUPPLEMENTARY DATA

Supplementary Data are available at NAR Online.

ACKNOWLEDGEMENTS

The authors wish to thank the National Key Research & Development Program of China, the National Natural Science Foundation of China, and the Science Fund for Creative Research Groups of the National Natural Science Foundation of China for supporting this work.

FUNDING

National Key Research and Development Program of China [2019YFA0905504, 2018YFA0901302]; National Natural Science Foundation of China [51821006, 51878638]. Funding for open access charge: National Natural Science Foundation of China [2019YFA0905504].
Conflict of interest statement. None declared.

REFERENCES

1. Le,C., Ann,R., David,C., Shuailiang,L. and,Robert. (2013) Multiplex genome engineering using CRISPR/Cas systems. *Science*, **339**, 819–823.
2. Mardis,E.R. (2011) A decade's perspective on DNA sequencing technology. *Nature*, **470**, 198–203.
3. Hogan,A.M., Rahman,A., Lightly,T.J. and Cardona,S.T. (2019) A broad-host-range CRISPRi toolkit for silencing gene expression in burkholderia. *ACS Synth. Biol.*, **8**, 2372–2384.
4. Li,L., Liu,X., Wei,K., Lu,Y. and Jiang,W. (2019) Synthetic biology approaches for chromosomal integration of genes and pathways in industrial microbial systems. *Biotechnol. Adv.*, **37**, 730–745.
5. Cranenburgh,R.M., Hanak,J.A.J., Williams,S.G. and Sherratt,D.J. (2001) *Escherichia coli* strains that allow antibiotic-free plasmid selection and maintenance by repressor titration. *Nucleic Acids Res.*, **29**, e26.
6. Kang,C.W., Lim,H.G., Yang,J., Noh,M.H., Seo,S.W. and Jung,G.Y. (2018) Synthetic auxotrophs for stable and tunable maintenance of plasmid copy number. *Metab. Eng.*, **48**, 121–128.
7. Wein,T., Hulter,N.F., Mizrahi,I. and Dagan,T. (2019) Emergence of plasmid stability under non-selective conditions maintains antibiotic resistance. *Nat. Commun.*, **10**, 2595.
8. Mignon,C., Sodoyer,R. and Werle,B. (2015) Antibiotic-free selection in biotherapeutics: now and forever. *Pathogens*, **4**, 157–181.
9. Y.,S.C. and Milinkovitch,M.C. (2005) Separate-component-stabilization system for protein and DNA production without the use of antibiotics. *BioTechniques*, **38**, 775–781.
10. Mairhofer,J., Cserjan-Puschmann,M., Striedner,G., Nobauer,K., Razzazi-Fazeli,E. and Grabherr,R. (2010) Marker-free plasmids for gene therapeutic applications–lack of antibiotic resistance gene substantially improves the manufacturing process. *J. Biotechnol.*, **146**, 130–137.
11. Hagg,P., de Pohl,J.W., Abdulkarim,F. and Isaksson,L.A. (2004) A host/plasmid system that is not dependent on antibiotics and antibiotic resistance genes for stable plasmid maintenance in *escherichiacoli*. *J. Biotechnol.*, **111**, 17–30.
12. Yadav,V.G., De Mey,M., Lim,C.G., Ajikumar,P.K. and Stephanopoulos,G. (2012) The future of metabolic engineering and synthetic biology: towards a systematic practice. *Metab. Eng.*, **14**, 233–241.
13. Xiao,Y., Bowen,C.H., Liu,D. and Zhang,F. (2016) Exploiting nongenetic cell-to-cell variation for enhanced biosynthesis. *Nat. Chem. Biol.*, **12**, 339–344.
14. Santos,C.N., Regitsky,D.D. and Yoshikuni,Y. (2013) Implementation of stable and complex biological systems through recombinase-assisted genome engineering. *Nat. Commun.*, **4**, 2503.
15. Nah,H.J., Woo,M.W., Choi,S.S. and Kim,E.S. (2015) Precise cloning and tandem integration of large polyketide biosynthetic gene cluster

using *streptomyces* artificial chromosome system. *Microb. Cell Fact.*, **14**, 140.
16. Li,L., Wei,K., Liu,X., Wu,Y., Zheng,G., Chen,S., Jiang,W. and Lu,Y. (2019) aMSGE: advanced multiplex site-specific genome engineering with orthogonal modular recombinases in actinomycetes. *Metab. Eng.*, **52**, 153–167.
17. Sabri,S., Steen,J.A., Bongers,M., Nielsen,L.K. and Vickers,C.E. (2013) Knock-in/Knock-out (KIKO) vectors for rapid integration of large DNA sequences, including whole metabolic pathways, onto the *escherichiacoli* chromosome at well-characterised loci. *Microb. Cell Fact.*, **12**, 60.
18. Qi,L.S., Larson,M.H., Gilbert,L.A., Doudna,J.A., Weissman,J.S., Arkin,A.P. and Lim,W.A. (2013) Repurposing CRISPR as an RNA-guided platform for sequence-specific control of gene expression. *Cell*, **152**, 1173–1183.
19. Wang,Y., Zhang,Z.T., Seo,S.O., Lynn,P., Lu,T., Jin,Y.S. and Blaschek,H.P. (2016) Bacterial genome editing with CRISPR-Cas9: deletion, integration, single nucleotide modification, and desirable "Clean" mutant selection in *clostridiumbeijerinckii* as an example. *ACS Synth. Biol.*, **5**, 721–732.
20. Bassalo,M.C., Garst,A.D., Halweg-Edwards,A.L., Grau,W.C., Domaille,D.W., Mutalik,V.K., Arkin,A.P. and Gill,R.T. (2016) Rapid and efficient one-step metabolic pathway integration in *e. coli*. *ACS Synth. Biol.*, **5**, 561–568.
21. Chung,M.E., Yeh,I.H., Sung,L.Y., Wu,M.Y., Chao,Y.P., Ng,I.S. and Hu,Y.C. (2016) Enhanced integration of large DNA into *e. coli* chromosome by CRISPR/Cas9. *Biotechnol. Bioengin.*, **114**, 172–183.
22. Klompe,S.E., Vo,P.L.H., Halpin-Healy,T.S. and Sternberg,S.H. (2019) Transposon-encoded CRISPR-Cas systems direct RNA-guided DNA integration. *Nature*, **571**, 219–225.
23. Vo,P.L.H., Ronda,C., Klompe,S.E., Chen,E.E., Acree,C., Wang,H.H. and Sternberg,S.H. (2020) CRISPR RNA-guided integrases for high-efficiency, multiplexed bacterial genome engineering. *Nat. Biotechnol.*, **39**, 480–489.
24. Strecker,J., Ladha,A., Gardner,Z., Schmid-Burgk,J.L., Makarova,K.S., Koonin,E.V. and Zhang,F. (2019) RNA-guided DNA insertion with CRISPR-associated transposases. *Science*, **365**, 48–53.
25. Kwon,J.B. and Gersbach,C.A. (2019) Jumping at the chance for precise DNA integration. *Nat. Biotechnol.*, **37**, 1004–1006.
26. Min,D., Cheng,L., Zhang,F., Huang,X.N., Li,D.B., Liu,D.F., Lau,T.C., Mu,Y. and Yu,H.Q. (2017) Enhancing extracellular electron transfer of *shewanella oneidensis* MR-1 through coupling improved flavin synthesis and metal-reducing conduit for pollutant degradation. *Environ. Sci. Technol.*, **51**, 5082–5089.
27. Thomas,S., Maynard,N.D. and Gill,J. (2015) DNA red recombination and I-SceI cleavage library constructionusing gibson assembly®. *Nat. Methods*, **12**, 1098.
28. Cheng,L., Min,D., He,R.L., Cheng,Z.H., Liu,D.F. and Yu,H.Q. (2020) Developing a base-editing system to expand the carbon source utilization spectra of *shewanella oneidensis* MR-1 for enhanced pollutant degradation. *Biotechnol. Bioeng.*, **117**, 2389–2400.
29. Hwang,S.Y., Nakashima,K., Okai,N., Okazaki,F., Miyake,M., Harazono,K., Ogino,C. and Kondo,A. (2013) Thermal stability and starch degradation profile of alpha-amylase from *streptomyces avermitilis*. *Biosci. Biotechnol. Biochem.*, **77**, 2449–2453.
30. Park,J.-U., Tsai,A.W.-L., Mehrotra,E., Petassi,M.T., Hsieh,S.-C., Ke,A., Peters,J.E. and Kellogg,E.H. (2021) Structural copies basis for targetsite selection in RNA-guided DNA transposition systems. *Science*, **373**, 768–774.
31. Yang,J., Sun,B., Huang,H., Jiang,Y., Diao,L., Chen,B., Xu,C., Wang,X., Liu,J., Jiang,W. *et al.* (2014) High-Efficiency scarless genetic modification in escherichia coli by using lambda red recombination and I-SceI cleavage. *Appl. Environ. Microbiol.*, **80**, 3826–3834.
32. Davy,A.M., Kildegaard,H.F. and Andersen,M.R. (2017) Cell factory engineering. *Cell Syst.*, **4**, 262–275.
33. Gelvin,S.B. (2017) In: Bonini,N.M. (ed). *Annual Review of Genetics*. Vol. **51**, pp. 195–217.
34. Gu,P., Yang,F., Su,T., Wang,Q., Liang,Q. and Qi,Q. (2015) A coupling improved flavin synthesis and metal-reducing conduit for pollutant degradation rapid and reliable strategy for chromosomal integration of gene(s) with multiple copies. *Sci. Rep.*, **5**, 9684.
35. Mahillon,J. and Chandler,M. (1998) Insertion sequences. *Microbiol. Mol. Biol. Rev.*, **62**, 725–774.
36. Heidelberg,J.F., Paulsen,I.T., Nelson,K.E., Gaidos,E.J., Nelson,W.C., Read,T.D., Eisen,J.A., Seshadri,R., Ward,N., Methe,B. *et al.* (2002) Genome MR-1 for enhanced pollutant degradation sequence of the dissimilatory metal ion-reducing bacterium *shewanella oneidensis*. *Nat. Biotechnol.*, **20**, 1118–1123.
37. Li,F., Li,Y.X., Cao,Y.X., Wang,L., Liu,C.G., Shi,L. and Song,H. (2018) Modular engineering to increase intracellular NAD(H/(+)) promotes rate of extracellular electron transfer of *shewanella oneidensis*. *Nat. Commun.*, **9**, 3637.
38. Li,F., Li,Y., Sun,L., Li,X., Yin,C., An,X., Chen,X., Tian,Y. and Song,H. (2017) The importance of porins engineering *shewanella oneidensis* enables xylose-fed microbial fuel cell. *Biotechnol. Biofuels*, **10**, 196.
39. Yang,C., Rodionov,D.A., Li,X., Laikova,O.N., Gelfand,M.S., Zagnitko,O.P., Romine,M.F., Obraztsova,A.Y., Nealson,K.H. and Osterman,A.L.(2006) Comparative pathways genomics and experimental characterization of N-acetylglucosamine utilization pathway of *shewanella oneidensis*. *J. Biol. Chem.*, **281**, 29872–29885.
40. Lowe,H., Sinner,P., Kremling,A. and Pfluger-Grau,K. (2020) Engineering overview sucrosemetabolism in pseudomonas putida highlights the importance of porins. *Microb. Biotechnol.*, **13**, 97–106.
41. Pastor,J.M., Borges,N., Pagan,J.P., Castano-Cerezo,S., Csonka,L.N., Goodner,B.W., Reynolds,K.A., Goncalves,L.G., Argandona,M., Nieto,J.J. *et al.* (2019) Fructose metabolism in chromohalobacter salexigens: interplay between the embden-meyerhof-parnas and entner-doudoroff pathways. *Microb. Cell Fact.***18**, 134.
42. Zhang,Q., Han,Y. and Xiao,H. (2017) Microbial mobile group II introns and their reverse transcriptases: gene targeting, RNA-seq, and non-coding RNA analysis α-amylase: abiomolecular overview. *Process Biochem.*, **53**, 88–101.
43. Kotloski,N.J. and Gralnick,J.A. (2013) Flavin electron shuttles dominate extracellular electron transfer by *shewanella oneidensis*. *Mbio.*, **4**, e00553-12.
44. Enyeart,P.J., Mohr,G., Ellington,A.D. and Lambowitz,A.M. (2014) Biotechnological applications of mobile group II introns transposons and their reverse transcriptases: genetargeting, RNA-seq, and non-coding RNA analysis. *Mobile DNA*, **5**, 2.
45. Peters,J.M., Koo,B.M., Patino,R., Heussler,G.E., Hearne,C.C., Qu,J., Inclan,Y.F., Hawkins,J.S., Lu,C.H.S., Silvis,M.R. *et al.* (2019) Enabling considerations genetic analysis of diverse bacteria with Mobile-CRISPRi. *Nat. Microbiol.*, **4**, 244–250.
46. Tellier,M., Bouuaert,C.C. and Chalmers,R. (2015) Mariner and the ITm superfamily of transposons. *Microbiol. Spectr.*, **3**, MDNA3-0033-2014.
47. McLellan,M.A., Rosenthal,N.A. and Pinto,A.R. (2017) Cre-loxP-Mediated recombination: general principles and experimental considerations. *Curr. Protoc. Mouse Biol.*, **7**, 1–12.
48. Horlbeck,M.A., Xu,A., Wang,M., Bennett,N.K., Park,C.Y., Bogdanoff,D., Adamson,B., Chow,E.D., Kampmann,M., Peterson,T.R. *et al.* (2018) Mapping the genetic landscape of human cells. *Cell*, **174**, 953–967.
49. Hickman,A.B. and Dyda,F. (2016) DNA transposition at work. *Chem. Rev.*, **116**, 12758–12784.
50. Kocak,D.D., Josephs,E.A., Bhandarkar,V., Adkar,S.S., Kwon,J.B. and Gersbach,C.A. (2019) Increasing the specificity of CRISPR systems with engineered RNA secondary structures. *Nat. Biotechnol.*, **37**, 657–666.